Translocation Properties of Novel Cell Penetrating Transportan and Penetratin Analogues

ARTICLE *in* BIOCONJUGATE CHEMISTRY · SEPTEMBER 2000

Impact Factor: 4.51 · DOI: 10.1021/bc990156s · Source: PubMed

Translocation Properties of Novel Cell Penetrating Transportan and Penetratin Analogues

Maria Lindgren,[†] Xavier Gallet,[‡] Ursel Soomets,[†,§] Mattias Hällbrink,[†] Ebba Bråkenhielm,[†] Margus Pooga,[†,||] Robert Brasseur,[‡] and Ülo Langel*[,†]

Department of Neurochemistry and Neurotoxicology, Arrhenius Laboratories, Stockholm University, S-106 91 Stockholm, Sweden, Centre de Biophysique Moléculaire Numérique, Faculté Universitaire des Agronomiques, Passage des déportés 2, 5030 Gembloux, Belgium, Department of Biochemistry, Tartu University, Ravila 19, 50411, Tartu, Estonia, and Estonian Biocenter, Riia 23, 51010, Tartu, Estonia. Received November 12, 1999; Revised Manuscript Received May 1, 2000

Novel analogues of the cell-penetrating peptides penetratin and transportan were synthesized. The distribution of the biotin-labeled peptides in Bowes melanoma cell line has been investigated by indirect fluorescence with fluorescein-streptavidin detection. The time course of uptake of ^{125}I-labeled transportan analogues has been characterized in the same cell line. Molecular modeling was used to analyze the penetration and the orientation of molecules in a simulated biological membrane. The results, both from molecular modeling and fluorescence studies, imply that penetratin and transportan do not enter the cells by related mechanisms and that they do not belong to the same family of translocating peptides.

INTRODUCTION

A number of techniques has been developed to deliver different cellular effectors into cells. The majority of techniques of delivery are invasive, like electroporation and microinjection. Liposome encapsulation and receptor-mediated endocytosis are milder methods, but also suffer from serious drawbacks, in particular, low delivery yield. As a new candidate with fewer drawbacks stands the class of transporting peptides with an ability to enter the cells in an energy-independent manner and also to bring certain macromolecules into the cells (for review see ref *1*).

Recently, a rapidly expanding family of peptide-based cellular transporters has been developed by several research groups. The initial work was carried out on a 16 amino acid long peptide derived from the third helix of the Antennapedia homeodomain protein crossing plasma membranes with high efficacy in an energy independent manner (*2*, *3*). This opened up new possibilities for the development of useful and efficient carrier vectors. Indeed, this peptide, the first member of the family of peptide transport vectors today known as penetratins, has now been shown to deliver small proteins, DNA (*4*), and PNA[1] oligomers into cells (*5*). Structure/function studies have been carried out on penetratin in order to define the structural requirements and the mechanism of the cell penetration and to improve the carrier efficacy of the peptides (*6*, *7*).

Transportan (*8*), a 27 amino acid long chimeric peptide, introduced by our group, is a combination of the N-terminal fragment of the neuropeptide galanin and the membrane interacting wasp venom peptide mastoparan. A Lys[13] residue connects these two bioactive peptides, and its ε-amino group is used for coupling of cargoes. Transportan, like penetratin, efficiently crosses plasma membranes in an energy independent manner (*8*).

In this paper, the two translocating peptides, penetratin and transportan, and their novel analogues, have been tested for their ability to enter Bowes melanoma cells by using indirect fluorescence and ^{125}I-labeled or fluorophor-labeled peptides. Additionally, molecular modeling was used to analyze the interaction of peptides with membranes. This theoretical approach reveals that penetratin and transportan may not insert into the phospholipid bilayer in the same manner and may have different orientation in the membrane.

EXPERIMENTAL PROCEDURES

Peptide Synthesis. The peptides were synthesized in a stepwise manner in a 0.1 mmol scale on a model 431A peptide synthesizer (Applied Biosystems) using *t*-Boc strategy of solid-phase peptide synthesis. *tert*-Butyloxycarbonyl amino acids were coupled as hydroxybenzotriazole esters to a *p*-methylbenzylhydrylamine (MBHA) resin (Bachem, Switzerland) to obtain C-terminally amidated peptides. Biotin was coupled manually to ε-amino group of Lys after orthogonal deprotection from Fmoc-group, using 3-fold excess of HOBt and TBTU activated biotin (Chemicon, Sweden) in DMF to the peptide on resin. Deprotection of the side chains from formyl and benzyl groups was carried out using the low TFMSA method. The peptides were cleaved with liquid HF at 0 °C for 30 min in the presence of *p*-cresol or thiocresol/*p*-cresol as scavengers when Met was present. The purity

* To whom correspondence should be addressed. Phone: 46-8-161793. Fax: 46-8-161371. E-mail: ulo@neurochem.su.se.
[†] Department of Neurochemistry and Neurotoxicology.
[‡] Centre de Biophysique Moléculaire Numérique.
[§] Department of Biochemistry.
[||] Estonian Biocenter.

[1] Abbreviations: PNA, peptide nucleic acid; HOBt, hydroxybenzotriazole, TBTU, 2-(1H-benzotriazole-1-yl)- 1,1,3,3- tetramethyluronium tetrafluoroborate, FITC; fluorescein-5-isothiocyanate, GRAVY; grand average of hydrophathicity, RAMSES; rapid analysis master/salves extensible system, MHP; molecular hydrophobic potentials, TFMSA; trifluoromethane sulfonic acid, HF; hydrofluoric acid, ER; endoplasmatic reticulum, ABZ; anthranilic acid, HKR; Hepes Krebs Ringer buffer.

10.1021/bc990156s CCC: $19.00
Published on Web 09/18/2000

Table 1. Comparison of Cell Penetrating Properties of Penetratin and Its Novel Analogues in Bowes Cells[a]

peptide	uptake indirect fluorescence
biotinyl-penetratin(1−16)-[$N^{1\alpha}$-biotinyl]-pAntp(43−58) (*6*), biotinyl-RQIKIWFQNRRMKWKK amide	+
[$N^{1\alpha}$-biotinyl]-[D-Pro^8]-ent-Penetratin−amide, biotinyl-all-D-RQIKIWFPNRRMKWKK amide	++
[$N^{1\alpha}$-biotinyl]-Arg-Phe-Trp-Ile-Asn-Lys−penetratin(8−16) amide, biotinyl-RFWINKQNRRMKWKK amide	+
[$N^{1\alpha}$-biotinyl, Leu^6]−penetratin, biotinyl-RQIKILFQNRRMKWKK amide	−
[bis-$N^{1\alpha}$−biotinyl,$N^{16\epsilon}$-penetratin (1-15)]−biotinyl-penetratin(1−16), biotinyl-RQIKIWFQNRRMKWK-[biotinyl-RQIKIWFQNRRMKWKK] amide	++

[a] Cells were incubated with 10 μM peptides at 37 °C for 60 min. The uptake efficiency is estimated fluorescence intensity and relative to the transportan original sequence [(++) comparable uptake to that of transportan, (+) a peptide with half the intensity compared to transportan, (−) no noticeable difference from control cells, that is without addition of peptide].

of the peptides was > 98% as demonstrated by HPLC on an analytical Nucleosil 120-3 C_{18} RP-HPLC column (0.4 × 10 cm). The molecular masses of the peptides were determined with a Plasma Desorption Mass Spectrometer (Bioion 20, Applied Biosystem) and the calculated values were obtained in each case.

Iodination. Peptide iodination was carried out by the chloramine T method (*9*). $Na^{125}I$ (specific activity 16.1 mCi/mg, concentration 0.1 mCi/mL) was mixed with 5 equiv of the peptides, and phosphate buffer was added in 10-fold excess. The chloramine T solution was prepared at a concentration of 2 mg/mL in phosphate buffer, pH 7.4. After 2 min of incubation, the reaction was stopped by adding sodium metabisulfit (2.4 mg/mL in phosphate buffer, pH 7.4). The peptides were purified on a reversed-phase, RP, column SEP-PAK 51910 (Millipore) using stepwise gradient of acetonitrile in water. The iodination was performed using 1 mCi $Na^{125}I$ and 4.9 nmol of biotinylated peptide for transportan and transportan 2, while transportan 3 was iodinated using 5 mCi of $Na^{125}I$ and 12.6 mmol, respectively. The fractions with the highest specific activity of radiolabeled peptides were used in the experiments.

Cells. The human Bowes melanoma cell line was cultivated in minimal essential medium with Earl-salts (MEM) supplemented with 10% foetal calf serum, 2 mM L-glutamine, 100 IU/mL penicillin and 100 μg/mL streptomycin in air with CO_2 enriched to 5% at 37 °C. Bowes cells were grown on round glass coverslips in a 24 well plate to approximately 50% confluence.

Cellular Penetration of Biotinyl-Labeled Peptides. The medium containing serum was exchanged for a serum-free medium, and a water solution of the biotinyl-peptides was added directly into the medium. The cells were then incubated for different time periods in 5% CO_2 enriched air at 37 °C. The cells were washed twice with PBS, fixed, and permeabilized with methanol for 10 min at −20 °C, washed again with PBS, and incubated for 1 h in a 5%(w/v) solution of bovine serum albumin in PBS in order to decrease unspecific binding. The peptides were visualized by staining with streptavidin-FITC (Amersham, U.K.) in the same solution for 1 h at room temperature. The cell nuclei were stained with Hoechst 33 258 (0.5 μg/mL) for 5 min, after which the coverslips were washed five times with PBS and mounted in 20% glycerol in PBS. As an control the same procedure was performed with an alternative fixation method: 3% *p*-formaldehyde in PBS 15 min and then pearmabilised for 3 min on ice with 30 mM Hepes buffer with 0.5% Triton X-100 (Sigma). This was done to distinguish membrane associated peptides from internalized peptides. The images were obtained by Zeiss Axioplan 2 microscope (Carl Zeiss Inc., Germany) equipped with a cooled digital CCD camera C4880 (Hamamatsu Photonics, Japan) or by a laser scanning confocal microscope (model LSM 510; Carl Zeiss Inc., Sweden) equipped with an Ar laser (488 nm), a He/Ne laser (543 nm), a 63 × 1.4 oil immersion objective. The Ar and He/Ne lasers were operated at 8 and 60% power, respectively. Images were processed using Adobe Photoshop 3.0 software (Adobe systems Inc., CA).

Cellular Penetration of ^{125}I-Labeled Peptides. Bowes cells were grown to 70−80% confluence in 75 cm^2 flask. The cells were scraped off and centrifuged at 1500 rpm for 10 min. The supernatant was discarded and the pellet resuspended in 2 mL of Hepes-buffered Krebs Ringer solution (HKR), pH 7.4 (5 mM Hepes, 137 mM NaCl, 2.68 mM KCl, 2.05 mM $MgCl_2 \cdot 6H_2O$, 1.8 mM $CaCl_2 \cdot 2H_2O$) with the addition of 1 mg/mL BSA. The cell suspension was aliquoted and the iodinated peptides were added to reach an activity of 1 million cpm/tube. The samples were incubated in a water bath at 37 °C up to 240 min. The samples were centrifuged through a mixture of 40% dioctylphthalate and 60% dibutylphthalate. The fractions were counted in γ-counter (Packard). Penetration of $Na^{125}I$ into Bowes cells was measured to estimate the intactness of cells and nonspecific binding.

Comparison of Transportan and Penetratin Uptake. Approximately 70.000 detached Bowes cells were incubated in HKR containing 10 μM ABZ-labeled peptides for 30 min in 37 °C and subsequently treated with 0.25% trypsin for 4 min to remove surface-bound peptide. The cells were harvested by centrifugation and washed twice. The fluorescence intensity was measured in a Hitachi F-2000 fluorescence spectrophotometer. As a control, peptides treated with trypsin prior to incubation with the cells, were used.

Prediction Programs. The characteristics presented in Table 3 are calculated using Prot Param prediction program (*10*). Statistical analysis of 44 proteins has revealed that there are certain dipeptides that occur in proteins in correlation with the stability of the protein (*11*). A weight value of instability to each of the 400 different dipeptides has been assigned. Using these weight values it is possible to compute an instability index (*11*). A protein whose instability index is smaller than 40 is predicted as stable, a value above 40 predicts that the protein may be unstable.

The estimated half-life is based on the findings that the N-terminal amino acid residue of a peptide plays an important role in determining its ubiquitin-mediated proteolytic stability in vivo (*12*−*14*). The set of individual amino acids can thus be ordered with respect to the half-lives that they confer when present at the amino terminus of a protein.

Table 2. Comparison of Cellular Uptake and Localization of Novel Transportan Analogues in Bowes Cells[a]

name	uptake indirect fluorescence
[$N^{13\varepsilon}$-biotinyl]transportan (*8*), GWTLNSAGYLLGK[biotinyl]INLKALAALAKKIL amide	++
[$N^{13\varepsilon}$-biotinyl]transportan 2, [GWTLNSAGYLLGK[biotinyl]INLKAKAALAKKLL amide[b]	++
[$N^{9\varepsilon}$-biotinyl]transportan 3, $C_6H_5CH_2CO$-Y(Me)FQNRPRYK[biotinyl]-(Ahx)[c]-INLKALAALAKKIL-amide	+
[$N^{13\varepsilon}$-biotinyl]transportan 4, GWTLNSAGYLLGK[biotinyl]FLPLILRKIVTAL amide[d]	−
[$N^{13\varepsilon}$-biotinyl,Pro^6]transportan or transportan 5, GWTLNPAGYLLGK[biotinyl]INLKALAALAKKIL amide	+
[$N^{13\varepsilon}$-biotinyl,Pro^6,Pro^7]−transportan or transportan 6, GWTLNPPGYLLGK[biotinyl]INLKALAALAKKIL amide	+

[a] Cells were incubated with 10 μM peptides at 37 °C for 60 min. The uptake efficiency is estimated and relative to the transportans original sequence [(++) comparable uptake to that of transportan, (+) a peptide with half the intensity compared to transportan, (−) no noticeable difference from control cells, that is without addition of peptide]. [b] Mas17, inactive mastoparan analogue, INLKAKAALAKKLL amide. [c] Synthetic vasopressin antagonist, $C_6H_5CH_2CO$−Y(Me)FQNRPRY, Ahx 6-aminohexanoic acid. [d] Membrane associating hornet venom crabrolin, FLPLILRKIVTAL amide.

Table 3. Physicochemical Properties of Penetratin and Transportan and the Improved Analogue Transportan 2[a]

characteristics	penetratin	transportan	transportan 2
1. no. of amino acids	16	27	27
2. pI	12.31	10.18	10.30
3. no. of charged amino acids	7+/0-	3+/0-	5+/0-
4. maximal reported cargo	55-mer DNA oligo (*4*)	21-mer PNA (*5*)	biotin
5. estimated half-life (in mammalian reticulocytes, in vitro) (h)	1	30	30
6. aliphatic index	48.75	148.52	134.07
7. GRAVY	−1.731	0.633	0.322
8. instability index	46.6	0.04	−7.09

[a] Prediction program ProtParam (http://expasy.hcuge.ch/cgi-bin/protparam) has been applied in calculations (*10*).

By statistical analysis (*15*), it has been shown that the aliphatic index, which is defined as the relative volume of a protein occupied by an aliphatic side chain, is significantly higher for proteins of thermophilic bacteria as to proteins found in other species. The aliphatic index may be regarded as a positive factor for the increase of thermostability of globular proteins.

GRAVY (*16*) or grand average of hydropathy values for a protein is achieved by sum the hydropathy values of all the amino acids and dividing by the number of residues in the sequence. The GRAVY score differs significantly for membrane embedded (high values), membrane bound and soluble proteins (usually negative values).

Membrane Interaction Modeling. The structure of each peptide (Tables 1 and 2) was predicted using the Stereo alphabet procedure. To each of the *n* amino acids of the sequence, six pairs of (ϕ,ψ) angles were attributed: −60°,−40° (right α-helix); −160°,160° (β-sheet); −140°,-80° (intermediary structure between β-sheet and 3^{10} helix); −80°,160° (helix of the polyproline); −80°,80° (3^{10} helix), and 60°,60° (left. α-helix). These structures correspond to the minimal energy states of an alanine residue on the van der Waals and electrostatic energy maps (*17*). The energy of each of the 6^n combinations was calculated and the conformations of minimal energy were recorded. They were submitted to a Simplex minimization procedure. This calculation was carried out in a medium of intermediate dielectric constant of a hydrophobic/hydrophilic interface (*18*). Nonpeptidic parts of molecules (biotin, amide group) were added using the Hyperchem 5.0 software (Autodesk, Sausalito, Ca).

In the Impala procedure (*19*), an empirical function *C* is used to describe the water−lipid interface. Considering that the properties of the membrane are constant in the plane of the bilayer, *C* varies along the *z* axis, normal to the lipid bilayer and has its origin ($z = 0$) at the center of the membrane.

$$C(z) = 1/[1 + \exp[\alpha(|z| - z_o)]]$$

With α and z_o defined so that $C \approx 1$ for $z < 18.5$ and $z > 18.5$ and $C \approx 0$ for $-13.5 < z < 13.5$. The interaction between the peptides and the lipids are described by the sum of two restraint functions:

$$E_{int} = -\sum_{(i=1,n)} S_i E_{tr_i} C(z_i)$$

E_{int} simulates the hydrophobic effect depending on the accessible surface of the peptides, and S_i is the atomic free energy of transfer from a hydrophobic to a hydrophilic phase E_{tr_i} and the position z_i of each atom *i*.

The second term mimics the solvophobic effect in the lipid phase:

$$E_{lip} = a_{lip} \sum_{(i=1,n)} S_i C(z_i)$$

where a_{lip} is an empirical constant.

The term E_{lip} tends to minimize the interactions between the peptide and the lipid if they are not as favorable as lipid/lipid interactions are. The conformation of peptides was fixed and their position and orientation were tested by running a Monte Carlo procedure of 10^5 steps at 310 K. Maximal rotations of 5 °C and translations of 1 Å were allowed. The Tammo procedure (*19*) was used to calculate the starting position of peptides at a single water/lipid interface taking into account the hydrophobic and the hydrophilic center of molecules. The peptide orientation of minimal energy was retained.

Calculations were performed on RAMSES (Rapid Analysis Master/Salves Extensible System), parallel hardware of 21 Tracor Europa Pentium Pro PC connected by a 100 megabyte network and controlled by a HP Vectra VA Pentium Pro. The calculation software have been developed in our laboratory (*19*). Molecular visualizations were

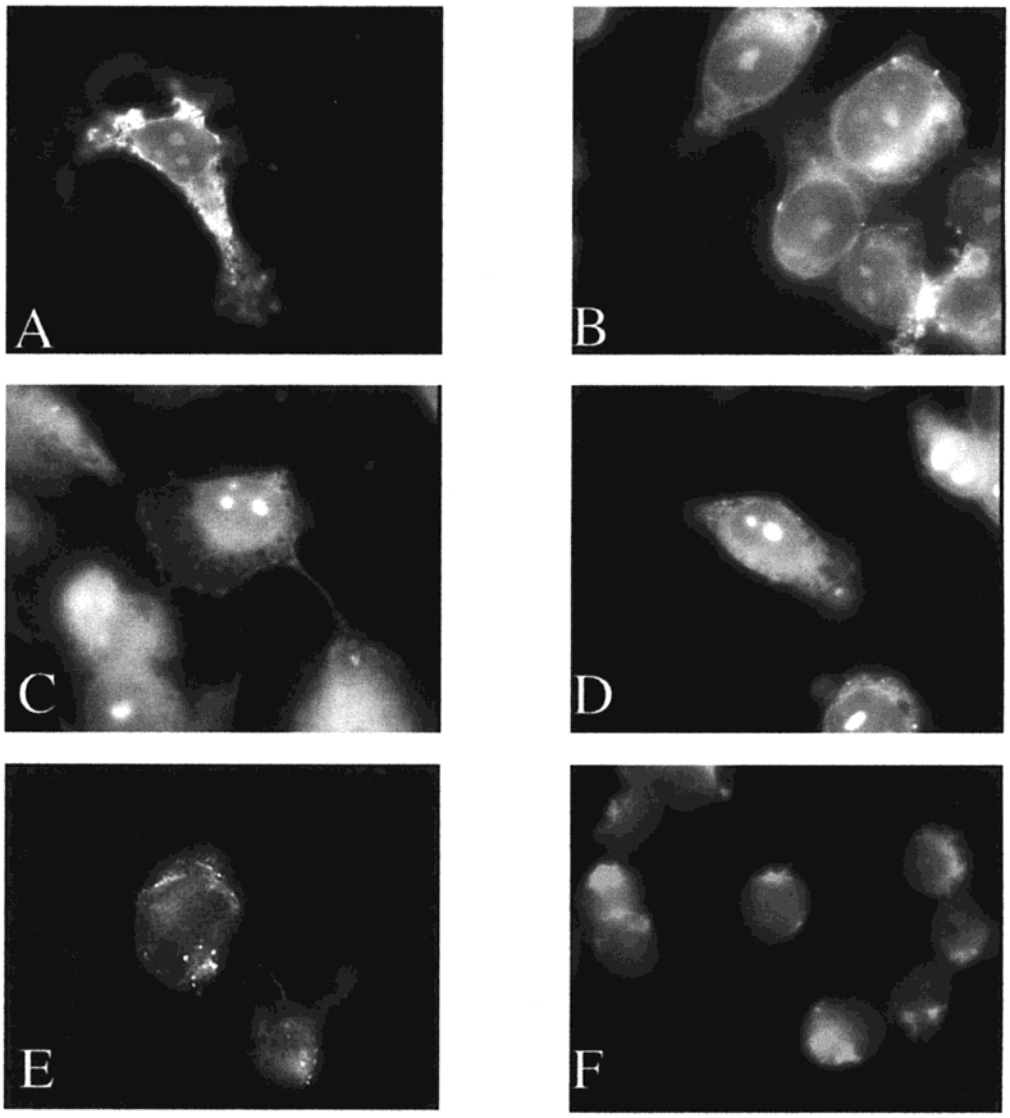

Figure 1. Internalization of biotinyl-peptides, by Bowes melanoma cells visualized by staining with streptavidin-FITC. Cells were incubated with 10 μM peptides for 30 min. (A and B) Transportan at 37 and 4 °C, respectively. (C and D) Penetratin at 37 and 4 °C, respectively. (E) transportan 3 at 37 °C and (F) control cells without any peptide added.

performed using WinMGM 2.0 software (*20*) from Ab Initio Technology (Obernai, France).

RESULTS

The new biotinyl-penetratin analogues [$N^{1\alpha}$-biotinyl]-[D-Pro^8]-*ent*-penetratin and [$N^{1\alpha}$-biotinyl-$N^{16\epsilon}$-penetratin-(1−15)]-penetratin(1−16) showed somewhat higher intracellular concentrations as judged by fluorescence microscopy of bound streptavidin-FITC than the biotinyl-penetratin(1−16) (Table 1).The peptides [$N^{1\alpha}$-biotinyl]-Arg-Phe-Trp-Ile-Asn-Lys-penetratin(8−16) and [$N^{1\alpha}$-biotinyl,Leu^6]-penetratin showed detectable but lower intracellular concentrations (Table 1).

All the new transportan analogues, except transportan 4 (Table 2), were also found to translocate into Bowes cells, both at 4 and at 37 °C. The peptides seem to associate with intracellular membranous structures, such as the ER and Golgi, but were also detectable in the cytosol. Transportan 3 treated cells had somewhat lower fluorescent signal as compared to transportan, while transportan 2 showed a comparable signal (Table 2). These data are in accordance with data obtained with iodinated peptides (Figure 2). Transportan 4 had the lowest penetration capability of all the peptides in this study.

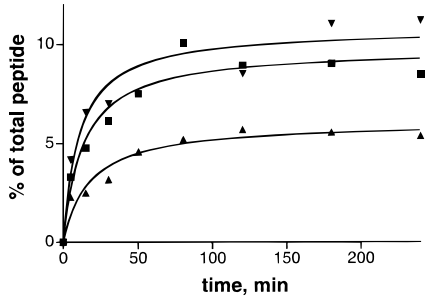

Figure 2. Cellular uptake of [^{125}I]transportan and its [^{125}I]-analogues into Bowes melanoma cells. Cells were incubated at 37 °C with 10 nM [^{125}I]transportan (■), 10 nM [^{125}I]transportan 2 (▼), 10 nM [^{125}I]transportan 3 (▲). Points are experimental; curves were fitted with the aid of the nonlinear regression program (GraphPad Software, Inc.).

The two transportan analogues with proline substitutions did give weaker staining than the original peptide but comparable signal to transportan 3. The order of cellular uptake by immuno fluorescence was transportan

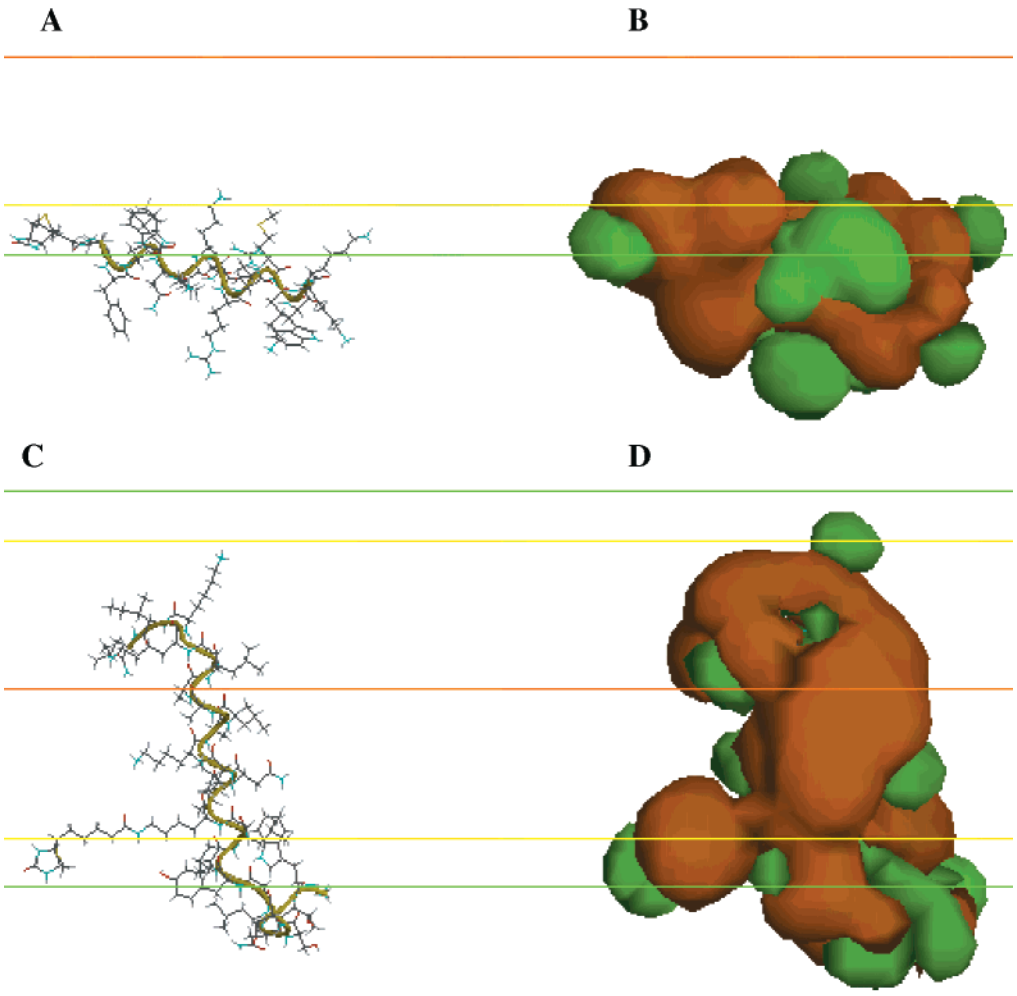

Figure 3. Interaction of calculated peptides with a membrane model. The orange line denotes the center of the bilayer ($z = 0$). Yellow line ($z = 13.5$ Å), green line ($z = 18$ Å). The environment is completely hydrophilic bellow the green line and completely hydrophobic above the yellow line. (A) Orientation of [$N^{1\alpha}$-biotinyl]Arg-Phe-Trp-Ile-Asn-Lys-penetratin(8−16) parallel to the membrane surface. The yellow ribbon shows the secondary structure of the peptide. (B) Calculation of the molecular hydrophobic potentials, MHP, around this peptide in the same orientation as in panel A. Orange surfaces are associated with hydrophobic isopotentials and green patches with hydrophilic isopotentials domains. (C) Orientation of [$N^{13\epsilon}$-biotinyl]transportan normal to the membrane surface. (D) Calculation of MHP around the peptide in the same orientation as in panel C.

and transportan 2 > transportan 3, transportan 5, and transportan 6 > transportan 4.

Peptide iodination on tyrosine was successfully carried out with transportan, transportan 2 and transportan 3, the peptides with demonstrated cellular localization (cf. above). The time courses of the uptake of [^{125}I]transportan, −2, −3 by Bowes melanoma cells are shown in Figure 2. All [^{125}I]transportans are internalized even at 10 nM concentration and time courses of cell penetration of the peptides are comparable. The maximum uptake for labeled transportan and transportan 2 are nearly identical, 9.8 ± 0.6 and 10.7 ± 0.8% of total peptide, respectively, while the same value for transportan 3 is significantly lower, 6.0 ± 0.4% of total peptide added. The efficiency and time course of uptake are in accordance with earlier result shown for transportan (*8*).

The ABZ-labeled transportan and penetratin were used to compare the amount of internalized peptide at equilibrium. The amount of internalized peptide corresponded to 6.7 ± 0.3% for transportan and 3.3 ± 0.4 for penetratin of the total added peptide thus the cellular concentration of transportan should be about two times higher than for penetratin, this is in accordance with the immunofluorecsence data (Figure 4).

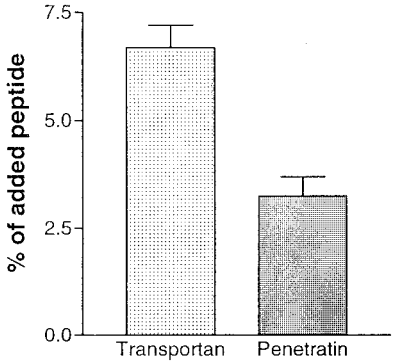

Figure 4. Percent of added transportan and penetratin.

In fluorescence studies, it was earlier shown (*21*) that using a strong fixative such as methanol could cause diffusion of internalized small molecules such as peptides. Therefore, the alternative formaldehyde fixative should be used to better preserve the cells internal structure and peptide localization as compared to nonfixed cells. Therefore both protocols for fixation of cells were used in this study, and they did give the same result.

Comparison of Penetratin and Transportan. Both penetratin and transportan enter the cells with high

efficiency but the staining pattern with FITC-streptavidin (Figure 1) is somewhat different. The plasma membrane is visualized by both peptides while the nuclear membrane staining is visible with transportan only. Penetratin does show nuclear localization, as do all the penetratin analogues, but has an more diffuse staining of the cell interior. It is possible that transportans higher affinity for cellular membrane structures could allow the membranes to act as a sink for the peptide which would explain its higher intracellular concentration.

Both penetratin and transportan internalize in an energy independent manner (Figure 1.). They have more common properties than that of cellular uptake but they also differ in several. Penetratin is a part of a protein while transportan is a synthetically combined sequence of two biologically active naturally occurring peptides, which may explain their differences in stability (see Table 3). Penetratin is 16 amino acids long while transportan is 27, although shorter penetratin contains almost the double amount of basic/positively charged residues, which are known to be cleavage sites for proteases.

Results from the ProtParam prediction programs (*10*) give the half-life of degradation for transportan to 30 h in eucaryotic cells, while the corresponding value for the penetratin sequence is only 1 h. The great difference in estimated stability should be taken into consideration when choosing a transporting peptide for a certain application.

The GRAVY values (Table 3) (*16*) suggest that the penetratin sequence would not be found in a membrane-spanning part of the protein while transportan is in the GRAVY range of integral membrane proteins such as the rhodopsins (0.70 for bacteriorhodopsin and 0.28 for bovine rhodopsin). This, and the fact that transportan is a hydrophobic peptide, would explain transportans localization into membranous structures such as ER and the Golgi.

In the membrane interaction model, penetratin was rejected out of the bilayer while transportan spanned the membrane with an angle of 65° to the surface plane (Figure 3). In contrast, both peptides do enter the cells, as shown by fluorescence, iodination, and various biological effects. The great difference in physicochemical properties of transportan and penetratin, and the fact that they both do penetrate into cells, support the idea of these two peptides translocating the plasma membrane in different manner.

Penetratin has been shown to deliver a 55 nucleotide long DNA oligomer (*22*) into cells while transportan has internalized with a 21mer of PNA, as cargo (*5*). The cargo size limit of both the peptides remains to be determined.

Membrane Interaction. Molecular modeling studies were performed on five sequences of penetratin (Table 1) and four sequences of transportan (Table 2). Modeling of secondary structure of peptides reveal that, peptides adopt an α-helical conformation although their end parts have a coiled structure, particularly for the N-terminus of [$N^{13\epsilon}$-biotinyl]transportan, transportan 2 and 4. This conformation is probably determined by the orientation of the bulky tryptophan side chain.

Among the five analogues of penetratin tested with the Impala procedure, two peptides, biotinyl-penetratin(1−16) and [bis-$N^{1\alpha}$-biotinyl,$N^{16\epsilon}$-penetratin(1−15)]-penetratin(1−16), were rejected out of the lipid bilayer. The most stable position of the [$N^{1\alpha}$-biotinyl]-[D-Pro^8]-ent-penetratin peptide is an oblique orientation according to the membrane plane. Its N-terminal end including the biotinyl group is buried into the apolar phase when the main part of the peptide is located out of the bilayer. The peptide [$N^{1\alpha}$-biotinyl]Arg-Phe-Trp-Ile-Asn-Lys-penetratin(8−16) lies flat at the membrane interface pointing some polar and charged side chains (Arg1, Gln7, Asn8, and Lys14) toward the area corresponding to the phospholipid polar heads (Figure 3A). The [$N^{1\alpha}$-biotinyl, Leu^6]-penetratin peptide remains out of the membrane. It adopts an oblique orientation and only its N-terminal part (Arg1, Gln2, Ile3, and Arg10) interacts with the bilayer.

The most surprising result was obtained for the [$N^{13\epsilon}$-biotinyl]transportan which span the membrane with an angle of 65° with regard to the surface plane (Figure 3C). Only a part of the N-terminal end (Thr3 to Gly8) remains out of the bilayer, when the aromatic side chain (Trp2 and Tyr9) are located at the membrane interface. Calculation of molecular hydrophobic potentials [(MHP (*23*)] displays a rather hydrophilic N-terminal side (Figure 3D). The transportan 2 peptide lies flat at the interface between the phospholipid polar heads and the hydrophobic core, with most of the polar residues pointing toward the membrane outside. Due to its unusual structure (two peptides separated by an alkyl chain), the transportan 3 peptide displays a specific orientation. The N-terminal part with its four aromatic groups remains out of the membrane when the C-terminal peptide lies in the hydrophobic core, pointing its three lysine residues into the phospholipid polar heads area. The transportan 4 peptide is slightly tilted with regard to the membrane interface. It lies in the area corresponding to the phospholipid heads with an angle of 22°.

The presence of proline residues gave a kinked helical structures to [$N^{1\alpha}$-biotinyl]-[D-Pro^8]-ent-penetratin and [$N^{13\epsilon}$-biotinyl]transportan 4. The proline analogues have coiled structure in the N-terminal domain due to the helix-breaker ability of the proline residues. Nevertheless, this conformation is stabilized in the transportan 5 by π-stacking interactions between the aromatic side chains of tyrosine and tryptophane residues. At the C-terminal ends of transportan 5 and transportan 6, the carbonyl group interacts with the amino group of the last but one lysine residue according to the running sequence. Due to the sequence similarity the proline analogues, transportan 5 and transportan 6, exhibit almost identical orientations in the membrane interaction model. They span the phospholipid leaflets with angles of 54 and 76°, respectively. For both molecules, the biotinyl group, the polar (Thr3, Asn5) and aromatic (Trp2, Tyr9) residues in the N-terminal end lay in the phospholipid polar heads area when the Lys25 residues is anchored in the opposite equivalent area. The α-helical content of the proline analogues were estimated to be much lower than compared to the other peptides in this study, thus the helix breaker, proline, had a great influence on internalization of the transportan peptide. This is in agreement with Scheller et al. (*24*) who showed that the amphilicity of the α-helix is of great importance for cellular penetration.

DISCUSSION

In view of the fact that the intracellular concentrations of [$N^{1\alpha}$-biotinyl,Pro^8]-penetratin, where glutamine has been substituted with a proline residue, and of the D-amino acid analogue were somewhat higher as compared to the original peptide, a new analogue was designed containing both of these modifications. The resulting peptide, the [$N^{1\alpha}$-biotinyl]-[D-Pro^8]-*ent*-penetratin-amide, indeed showed the highest intracellular staining, followed by indirect immunofluorescence, of all of the penetratin analogues tested (Table 1) although this

cannot be interpreted unambiguously. The higher intracellular concentration could be a result of lower degradation because of the lack of lysozymes that can digest the peptide bonds between D-amino acids, and not of more effective internalization.

An all-D-amino acid peptide with the sequence RFWINK-amide was found by screening a peptide library for μ-opioid receptor agonists and found to exhibit long lasting opoid effects in vivo (*25*). This implicates that the peptide crosses the blood−brain barrier. Because of the similarities in amino acid contents between the first part of penetratin and the opioid agonist, the N-terminal was substituted in its L-amino acid form resulting in the [$N^{1\alpha}$-biotinyl]Arg-Phe-Trp-Ile-Asn-Lys-penetratin(8−16) amide. The uptake was rather low, but still it would be interesting to study by which degree this peptide, in its enantio form, can pass the blood-brain-barrier.

[$N^{1\alpha}$-biotinyl,Leu^6]penetratin was designed to test the significance of the aromatic residue tryptophan, which seems to be of great importance as the uptake was lowered, probably due to loss of the stabilizing Trp−membrane interaction (Figure 3).

Penetratin has been proposed to internalize as a dimer (*6*); therefore, the branched peptide, [bis-$N^{1\alpha}$-biotinyl,$N^{16\epsilon}$-penetratin (1−15)]-biotinyl-penetratin(1−16), was synthesized. Indeed, this peptide does show a higher intracellular concentration than the original sequence. Whether this is caused by the dimeric nature of the peptide or the two binding sites for streptavidin, which could lead to slower degradation and thereby would leave one binding site intact, is not clear.

Currently, a model has been proposed for the cell penetration of penetratin which also is thought to apply for a fragment of the Tat protein (*6*), another cell penetrating peptide. This model suggests that the basic residues in the peptide can engage in ionic interactions with the negatively charged phospholipids in the cell membrane, causing a local invagination in the plasma membrane leading to local reorganization of the lipid bilayer, resulting in the formation of inverted micelles. These would enclose the peptide and its cargo in a hydrophilic environment to finally release them on the cytosolic face of the membrane.

Polycationic sequences are considered to exert their membrane destabilizing activity by interacting with negatively charged phospholipids in the plasma membrane. This is considered to result in internalization of the cationic peptides, possibly by the mechanism of non specific absorptive mediated endocytosis. The approach of polycationization could thus be used for targeting peptides to the cytoplasm of cells with a high rate of absorptive endocytosis. The peptides' ability to disorganize biological membranes also explains why many polycationic peptides are cytotoxic at high concentrations. This is the main drawback of this family of cell penetrating peptides, consequently amphipathic peptide toxins may not be able to function as carriers by themselves, due to high cytotoxicity, but rather be part of larger chimeras, such as transportan.

Transportan (*8*) has been shown to cross the plasma membrane of all animal cell lines tested so far at both 37 and 4 °C, thus implicating that the transport of the peptide is neither energy dependent nor receptor mediated. The internalization of transportan is not blocked by endocytosis inhibitors such as phenylarsine oxide or hyperosmolar sucrose solution, and the maximal intracellular concentration is reached after about 20 min. Transportan has, moreover, been coupled to a 21-mer PNA and this construct has been shown to penetrate cells (*5*).

In the penetration studies performed, transportan and transportan 2 give comparable signals by indirect fluorescence (Table 2) and iodination (Figure 2). The difference between these peptides are the C terminal part where transportan 2 contains the inactive mastoparan analogue, Mas 17 (*26*).

In transportan 3, the galanin part of the peptide is exchanged by the synthetic vasopressin antagonist to elucidate the receptor dependency of the internalization. The peptide was primarily found in the plasma membrane but not in the nucleus nor in internal membrane structures (Figure 1). The transportan 4 did not enter the cells in any detectable amount, hence the mastoparan part with its ampiphatic properties seems to be of great importance for the ability of this type of peptides to translocate the cellular membranes. In conclusion, the novel cell-penetrating transportan analogues should contain the mastoparan part while the galanin part could be modified whitout complete loss of internalization activity.

The molecular-modeling analysis shows that the peptides may use different ways to penetrate into the membrane. In our calculations, biotinyl-penetratin(1−16) and [bis-$N^{1\alpha}$-biotinyl,$N^{16\epsilon}$-penetratin(1−15)]-penetratin(1−16) were unable to insert into the bilayer demonstrate due to that those peptides contain a large number of basic residues which make them extremely hydrophilic. As proposed above, an unusual interaction mechanism may exist between those residues and the negative charges of the phospholipid heads that allows penetratin to destabilize the membrane and to penetrate into its hydrophobic core. The information concerning their translocation is not included in their amino acid sequences and the issue should be addressed in further studies.

Due to their amphiphilic character, most of the α-helical peptides adopt a flat or a slightly oblique orientation with regard to the membrane interface. Indeed, for biotinyl-penetratin(1−16), [$N^{1\alpha}$-biotinyl]-[D-Pro^8]-ent-penetratin, [$N^{1\alpha}$-biotinyl]Arg-Phe-Trp-Ile-Asn-Lys-penetratin(8−16), [$N^{1\alpha}$-biotinyl,Leu^6]-penetratin and, especially, transportan 4, the polar and charged amino acids are located on one side of the helix. The difference of orientation for the first two penetratin analogues indicate that an inverted chirality and the introduction of a proline residue may drastically change their mode of penetration. Amphiphilic peptides are adsorbed on the membrane surface and could cross progressively the lipid bilayer. This character of some peptides is displayed by the calculation of MHP (Figure 3B).

The [$N^{13\epsilon}$-biotinyl]transportan spans the lipid bilayer entirely with regard to an angle of 65°. This peptide has the most hydrophobic sequence and encloses only four polar amino acids while penetratin contains seven arginine or lysine residues. Furthermore, aromatic residues (Trp2 and Tyr9) lie at the membrane interface and stabilize the peptide insertion.

To conclude, the different modifications of the chimeric transportan, such as Mas 17 in transportan 2 and the vasopressin antagonist part in transportan 3, do not alter the peptides ability to translocate, while modifications of the amphipathic α-helical C-terminal, as mastoparan substituted to crabrolin in transportan 4 do. Crabrolin is, like mastoparan, a hemolytic peptide toxin and it has been shown to form α-helical structure (*27*), but the differences in sequence are sufficient to eliminate the

cellular uptake. The low internalization of the two proline substituted analogues further suggest the importance of the C-terminal α- helical structure of transportan. The penetratin analogues, on the other hand, were modified in a different manner. The single amino acid modifications did not alter the penetration ability, except for the Trp replaced with Leu in [$N^{1\alpha}$-biotinyl,Leu^6]penetratin, which made the N-terminus interact with the bilayer. The all-D analogue would be a useful transporter peptide if a longer effect would be desired. Even though the bispenetratin, like all the penetratins, is relatively hydrophilic it does enter the cells. The membrane interaction model implies that transportan's arrangement and features of its amino acids will explain the translocating property, while the penetratin sequence does not reveal its mode of penetration. Thus, it seems that penetratin and transportan are not belonging to the same family of translocating peptides and that they do not enter the cells by identical mechanisms.

ACKNOWLEDGMENT

We would like to thank Cecilia Kut (Södertörn University) for her help in preparing the fluorescence microphotographs. This work was supported by the European Community Biotechnology, BI104-98-0227, by EU MAST III CT97-0156, Swedish Research Council for Engineering Sciences (TFR), the Swedish Research Council for Natural Sciences (NFR), and also by the Swedish Institute (Visby program). M.P. is also supported by the Estonian Science Foundation (ETF 4007). R.B. is Directeur de Recherche FNRS (Fonds National de la Recherche Scientifique). X.G. is supported by the Interuniversity Poles of Attraction Program—Belgian State, Prime minister's Office—Federal Office for Scientific, Technical and Cultural Affairs', contract no. P.4/03.

LITERATURE CITED

(1) Lindgren, M., Hällbrink, M., Prochiantz, A., and Langel, Ü. (2000) Cell penetrating peptides. *Trends Pharm. Sci.* 21, 99−103.

(2) Bloch-Gallego, E., Le Roux, I., Joliot, A. H., Volovitch, M., Henderson, C. E., and Prochiantz, A. (1993) Antennapedia homeobox peptide enhances growth and branching of embryonic chicken motoneurons in vitro. *J. Cell. Biol. 120,* 485−492.

(3) Perez, F., Joliot, A., Bloch-Gallego, E., Zahraoui, A., Triller, A., and Prociantz, A. (1992) Antennapedia homeobox as a signal for the cellular internalization and nuclear addressing of a small exogenous peptide. *J. Cell. Sci. 102*, 392−396.

(4) Prochiantz, A. (1996) Getting hydrophilic compounds into cells: lessons from homeopeptides. *Curr. Opin. Neurobiol. 6*, 629−634.

(5) Pooga, M., Soomets, U., Hällbrink, M., Valkna, A., Saar, K., Rezaei, K., Kahl, U., Hao, J.-X., Xu, X.-J., Wiesenfeld-Hallin, Z., Hökfelt, T., Bartfai, T., and Langel, Ü. (1998) Cell penetrating PNA constructs regulate galanin receptor levels and modify pain transmission in vivo. *Nat. Biotech. 16*, 857−861.

(6) Derossi, D., Joliot, A., Chassaing, G., and Prochiantz, A. (1994) The third helix of the Antennapedia homeodomain translocates through biological membranes. *J. Biol. Chem. 269,* 10444−10450.

(7) Derossi, D., Calvet, S., Trembleau, A., Brunissen, A., Chassaing, G., and Prochiantz, A. (1996) Cell Internalization of the Third Helix of the Antennapedia Homeodomain Is Receptor-independent. *J. Biol. Chem. 271,* 18188−18193.

(8) Pooga, M., Hällbrink, M., Zorko, M., and Langel, Ü. (1998) Cell penetration by transportan. *FASEB J. 12*, 67−77.

(9) Gavin, J. R., Roth, J., Jen, P., and Freychet, P. (1972) Insulin receptors in human circulating cells and fibroblasts. *Proc. Natl. Acad. Sci. U.S.A. 69*, 747−751.

(10) Appel, R. D., Bairoch, A., and Hochstrasser, D. F. (1994) A new generation of information retrieval tools for biologists: the example of the ExPASy WWW server. *Trends Biochem. Sci. 19*, 258−260.

(11) Guruprasad, K., Reddy, B. V. B., and Pandit, M. W. (1990) Correlation between stability of a protein and its dipeptide composition: a novel approach for predicting in vivo stability of a protein from its primary sequence. *Protein Eng. 4*, 155−161.

(12) Bachmair, A., Finley, D., and Varshavsky, A. (1986) In vivo half-life of a protein is a function of its amino-terminal residue. *Science 234*, 179−186.

(13) Ciechanover, A., and Schwartz, A. L. (1989) How are substrates recognized by the ubiquitin-mediated proteolytic system? *Trends Biochem. Sci. 14*, 483−488.

(14) Tobias, J. W., Shrader, T. E., Rocap, G., and Varshavsky, A. (1991) The N-end rule in bacteria. *Science 254*, 1374−1377.

(15) Ikai, A. (1980) Thermostability and aliphatic index of globular proteins. *J. Biochem. 88*, 1895−1898.

(16) Kyte, J., and Doolittle, R. F. (1982) A simple method for displaying the hydropathic character of a protein. *J. Mol. Biol. 157*, 105−132.

(17) Lins, L., Brasseur, R., De Pauw, M., J. P., V. B., Ruysschaert, J. M., Rosseneu, M., and Vanloo, B. (1995) Helix-helix interaction in reconstituted high-density lipoproteins. *Biochim. Biophys. Acta 1258*, 10−18.

(18) Brasseur, R., and Ruysschaert, J. M. (1986) Conformation and mode of organization of amphiphilic membrane components: a conformational analysis. *Biochem. J. 238*, 1−11.

(19) Ducarme, P., Rahman, M., and Brasseur, R. (1998) IMPALA: a simple restraint field to simulate the biological membrane in molecular structure studies. *Proteins 30*, 357−371.

(20) Rahman, M., and Brasseur, R. (1994) WinMGM: a fast CPK molecular graphics program for analyzing molecular structure. *J. Mol. Graphics 12*, 212−218.

(21) Pichon, C., Monsigny, M., and Roche, A.-C. (1999) Intracellular localisation of oligonucleotides: influence of fixative protocols. *Antisense Nucleic Acid Drug Dev. 9*, 89−93.

(22) Ojcius, D., and Young, J. D. (1991) Cytolytic pore-forming proteins and peptides: is there a common structural motif? *Trends Biochem. Sci. 16*, 225−229.

(23) Brasseur, R. (1991) Differentiation of lipid-associating helices by use of three-dimensional molecular hydrophobicity potential calculations. *J. Biol. Chem. 266*, 16120−16127.

(24) Scheller, A., Oehlke, J., Wiesner, B., Dathe, M., Krause, E., Beyermann, M., Melzig, M., and Bienert, M. (1999) Structural requirements for cellular uptake of α-helical amphipathic peptides. *J. Pept. Sci. 5*, 185−194.

(25) Dooly, C. T., Chung, N. N., Wilkes, B. C., Schiller, P. W., Bidlack, J. M., Pasternak, G. W., and Houghten, R. A. (1994) An all D-amino acid opioid peptide with central analgestic activity from a combinatorial library. *Science 266*, 2019−2022.

(26) Soomets, U., Hällbrink, M., Zorko, M., and Langel, Ü. (1997) From galanin and mastoparan to galparan and transportan. *Curr. Top. Pept. Protein Res. 2*, 83−113.

(27) Krishnakumari, V., and Nagaraj, R. (1997) Antimicrobial and hemolytic activities of crabrolin, a 13-residue peptide from the venom of the European hornet, *Vespa crabro*, and its analogues. *J. Pept. Res. 50*, 88−93.

BC990156S